Tribological behavior of orthopedic foams/artificial skin systems: the effect of morphology, mechanical properties and surface free energy

D.A.Silva*

* Centro de Química Estrutural, Instituto Superior Técnico, ULisboa, Lisboa, Portugal

ABSTRACT: The discomfort associated to the use of orthosis results mainly from friction between the coating material, in this case the foams, and human skin. Although, nowadays the use of such devices is common, there is few information concerning the influence of the properties of the foams in the tribological behavior of the orthosis.

In this study it was investigated the effect of the morphology, mechanical properties and surface free energy in the values of friction coefficients of orthopedic foams/artificial skin systems.

The artificial skin was characterized using different techniques such as, atomic force microscopy (AFM) for analyzing the topography and the sessile drop method to determine its wettability.

Seventeen different commercial orthopedic foams were selected, and characterized concerning the morphology of their cells by scanning electron microscopy (SEM), surface free energy from wetting measures (sessile drop method) and mechanical properties through compression-decompression tests.

Nanotribological tests were performed between the artificial skin and the foam, with the application of various loads.

The results show that the increase in cell size and in the Young's modulus of the foams leads to a reduction in friction coefficients. In contrast, the increase in the surface free energy origins an increase in the friction coefficient.

Key-words: friction, artificial skin, orthopedic foams, morphology, mechanical properties and surface free energy.

1. INTRODUCTION

Today, there is a wide range of specific devices that allow the recovery of absent or decreased function in individuals affected by certain motor disorders.

In this context arises the orthosis, which are external to the body and whose goal is to change functional or structural aspects of the patient musculoskeletal system.

These orthopedic devices, generally used temporary, intend to support, align, prevent or correct deformations, or to improve the function of movable parts of the body

There are several types of orthosis for different anatomical areas and with different functionalities.

The main limitation of these orthopedic appliances is based on a potential discomfort that might occur in the charge transfer areas between the individual's skin and the orthosis, which may lead to skin lesions. The discomfort is due to the friction occurring between the skin and the coating of the orthosis, which is related to the forces generated at the interface skin/orthosis.

In most of the orthosis, the contact area with the skin is covered with foam. This way the coating material has an important role in the performance of these devices. Several properties of the foams may affect the tribological behavior of the systems.

The aim of this study was to analyze the effect of morphology, mechanical properties and surface free energy on the values of the friction coefficients of orthopedic foams/ artificial skin systems.

2. MATERIALS AND METHODS

2.1 Materials

The artificial skin used, commercially known by VITRO-SKIN by *IMS Inc*, is a synthetic substrate that approximately mimics the surface properties of human skin. It consists of optimized protein and lipid components and is designed to have topography, pH, critical surface tension and ionic strength similar to human skin [1] [2].

The seventeen commercial foams studied were: three copolymer based on ethylene and vinyl acetate (EVA, *Geriatric* EVA and *Nora Lunairflex*), five copolymer based on polyethylene (blue *Multiform*, white *Multiform*, brown *Multiform*, orange *Multiform* and red *Multiform*), five polyethylene (white *Plastazote*, normal clear *Plastazote*, perforated clear *Plastazote*, clear *Pelite* and dark *Pelite*), two polyurethane (clear and dark Polyurethane) and two *Sensofte* (high and low thickness).

2.2 Methods

2.2.1 Hydration of the artificial skin

The artificial skin was prepared according to the procedure given by the supplier [3], in particular, it was hydrated in a chamber which environmental humidity was regulated by an aqueous solution of 15% glycerin (99.5%, *Panreac*) placed in the bottom.

2.2.2 Morphology/topography of the artificial skin

The structure of the skin surface was characterized and determined its roughness by the atomic force microscopy (AFM) (*Nanosurf Easyscan 2)*.

2.2.3 Wettability of the artificial skin and the foams

The wettability of the artificial skin and the foams was accessed by the sessile drop method using water (deionized and distilled in a Milli-Q system) and diiodometahane (99%, *Sigma-Aldrich*) drops of 2-4 μL. The drops were generated with a micrometric syringe and deposited on the foam's surface at room temperature, inside a saturated chamber. Contact angle evolution was monitored during 900 s using a video camera coupled to a microscope (Wild M3Z) and to a frame grabber (Data Translation DT3155). Image acquisition and analysis were carried out using ADSA-P software. Reported results correspond to the average of at least five experiments.

The surface free energy (γ_{SV}) of the artificial skin and the foams was determined, using the method of the geometric mean presented in the equation:

$$\boldsymbol{\gamma_{LV}(1+cos\,\theta) = 2\sqrt{\gamma_{SV}^{d}\gamma_{LV}^{d}} + 2\sqrt{\gamma_{SV}^{p}\gamma_{LV}^{p}}}\,,$$

where the γ_{LV} is the superficial tension of the liquid and, γ_{LV}^{d} and γ_{LV}^{p} are the

dispersive and polar components, respectively, of the superficial tension of the liquids. According to the literature their values are: γ_{LV}^{d}=21.3 mJ/m^2 and γ_{LV}^{p}=50.7 mJ/m^2 for water, and γ_{LV}^{d}= 49.99 mJ/m^2 and γ_{LV}^{p}=0.4 mJ/m^2 for diodomethane [4]. The polarity of the surfaces ($\gamma_{LV}^{p}/\gamma_{LV}$) also was calculated.

2.2.4 Cleaning of the foams

Previous to testing, the foams were cleaned. The cleaning process consisted of placing three samples of foams inside a beaker with a 70% ethanol solution, followed by manual stirring for five minutes. Then, the foam samples were dried at room temperature in vacuum for two hours (pressure 30 mmHg).

2.2.5 Morphology of the foams

The foams morphology was analyzed through images obtained by field emission gun scanning electron microscopy (FEG-SEM) (Jeol JSM-7001F). Samples were previously coated with gold. The size and the wall thickness of the cells of the foams were determined from the SEM images, using the image processing software *Fiji*.

2.2.6 Mechanical properties of the foams

To evaluate the mechanical behavior of the foams compression tests were performed. Three measurements were carried out per foam, with a compression speed of 1mm/s in a 2.25 cm^2 sample area.

2.2.7 Nanotribological tests between the artificial skin and the foams

Reciprocating pin-on-plate tests were performed in a nanotribometer (CSM Instruments), with a sliding distance of 1mm and 1Hz of frequency during 10 minutes. Four applied loads were used: 100, 150, 200 and 250 mN. The pins were the selected commercial foams and the plate was the artificial skin mounted in a spherical surface with a radius of 1.25 cm (Figure 1). At least three tests were performed per tribological condition.

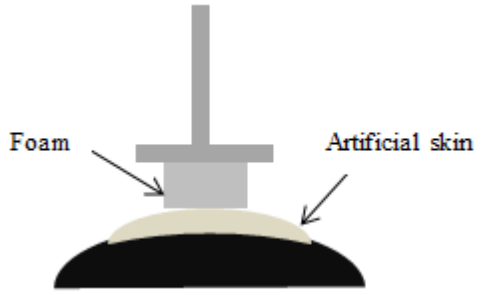

Figure 1. Representation of a nanotribological test.

3. RESULTS AND DISCUSSION

3.1 Morphology/topography of the artificial skin

Atomic force microscopy of the artificial skin allowed to observe in detail the structure of the surface, and determining its average roughness (R_a) (Figure 2). The obtained average roughness (R_a) was 54.3 ± 6 nm. According to the literature, the artificial skin has a much smaller roughness than human skin [5] [6], although this parameter is conditioned by the location of the skin in the body.

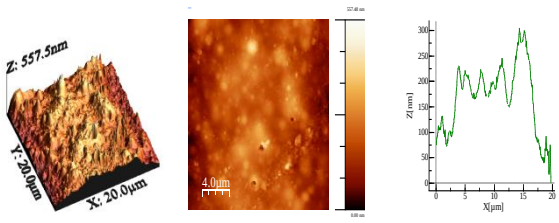

Figure 2. AFM image in 3D and 2D of the artificial skin and profile correspondent to the line presented in the 2D image.

3.2 Wettability of the artificial skin

Using the sessile drop method, the values of the contact angles between the artificial skin and two liquids (water and diodomethane) were obtained. Based on these, the surface free energy values were calculated (dispersive component, polar component and the total value), as well as the polarity of the artificial skin (Table 1).

Comparing with the human skin, the artificial skin presents higher surface free energy values [7] [8] [9].

Table 1. Contact angles of water and diiodomethane, the surface free energy (dispersive component, polar component and total) and polarity.

Θ_{Water} (°)	22 ± 4
$\Theta_{Diodomethane}$ (°)	42 ± 4
γ_s^d (mJ/m^2)	33 ± 2
γ_s^p(mJ/m^2)	36 ± 3
γ_s(mJ/m^2)	70 ± 2
Polarity	0.52 ± 0.04

3.3 Effect of the density of the foams in the Young's modulus

Three polyethylene foams, commercially named by *Plastazotes*, with closed cell structure, were compared.

Since the foams are cellular materials, the relative density (ρ / ρ_s) was calculated, being ρ the density of the foam and ρ_s the density of the bulk polyethylene (0.925 g/cm^3) [10]. The Young's modulus was also considered in relative terms (E / $E_{s)}$, in which the Young's Modulus of the bulk polyethylene (E_s) is 300 MPa [11].

It was verified that there is a direct relationship between the relative density and the relative Young's modulus of the foams, i.e., when the density increases, the Young's modulus also increases, which is in agreement with the literature [12]. So, white *Plastazote*, which presents the greater relative density, has the highest values of relative Young's modulus (Figure 3).

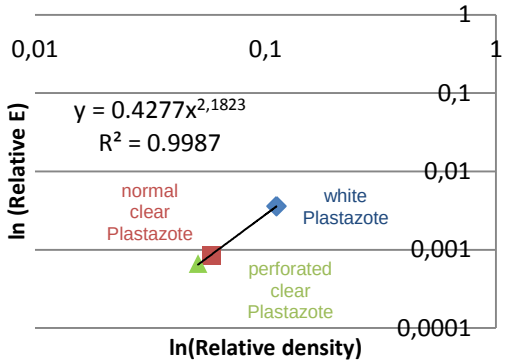

Figure 3. Representative graph of the relative Young's modulus depending on the relative density of Plastazote foams.

3.4 Effect of the cell size in wettability

Five polyethylene foams, three *Plastazotes* and two *Pelites*, all with closed cell structure and different cell radius size, were analyzed (Table 2).

The wettability results of the polyethylene foams showed that the contact angles were not very sensitive to foam cell size. Also, it was observed that the contact angles slightly decrease with the increase of the real contact area, between the polyethylene foams and water (Figure 4).

The foams are closed cell, resulting in air entrapment within the cells, which reduces the contact between the water and polyethylene. Water contact angles higher than those of solid polyethylene are expected. In fact, the literature reports contact angles between water and flat polyethylene surfaces in the range 90°-98° [13] [14], while obtained values of the

contact angles on the polyethylene foam are between 117° and 132°.

Table 2. Cell radius, contact angles with water and contact area for Polyethylene foams

Foams	Cell radius (µm)	Contact angles with water (°)	Contact area in 1 cm^2 (cm^2)
clear Pelite	82 ± 14	123 ± 2	0.02
dark Pelite	75 ± 11	117 ± 2	0.04
white Plastazote	78 ± 8	126 ± 6	0.02
normal clear Plastazote	127 ± 18	127 ± 4	0.01
perforated clear Plastazote	133 ± 21	132 ± 7	0.01

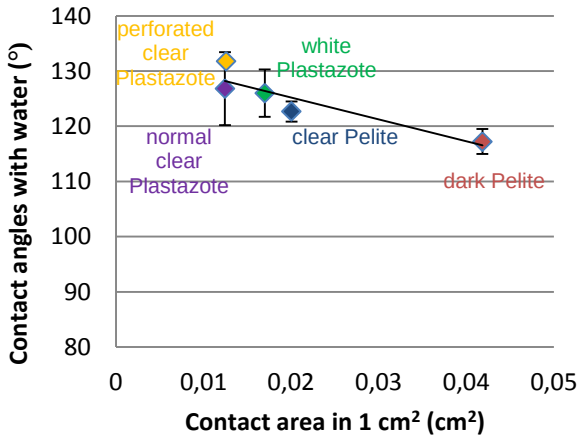

Figure 4. Representative graph of the water contact angles depending on the contact area in 1 cm^2

3.5 Effect of the adhesion in the nanotribological tests

When the tests are performed at a reduced scale, particularly in the nanotribology, there is preponderance of the adhesive forces in relation to applied normal forces [15].The adhesion force is mainly due to two factors: the surface free energy of interfaces, that is, the molecular nature of the adhesive bonds (Van der Waals, electrostatic, hydrogen and hydrophobic), and the contact area, where are established these bonds [16].

This consideration is related to the results presented in the following sections.

3.5.1 Effect of the normal applied load in the friction coefficient

Nanotribological tests were performed between the hydrated artificial skin and the foams, using four different forces (100, 150, 200 and 250 mN) (Figure 5).

The coefficient of friction decreases with increasing of the applied load for all the studied foams. This behavior has been extensively found in literature [17] [18] [19] [20].This result is due to the fact that for low loads, the adhesion forces play an important role in tangential force (friction force), thus leading to a proportional increase in friction coefficient [21].

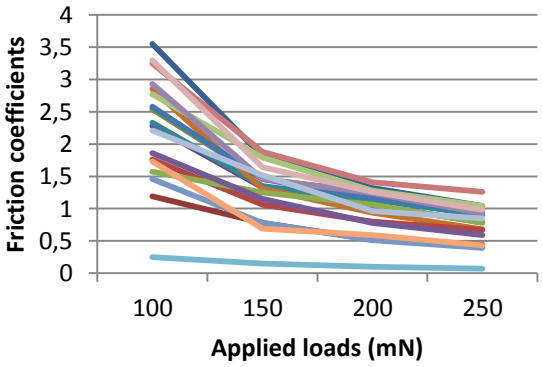

Figure 5. Variation of the friction coefficients with the applied load on the seventeen foams

For all foams the friction coefficient vs applied normal load was adjusted a power function ($\mu = k * Fn^N$), where µ is the friction coefficient, Fn is the total normal load, k is a load-dependent coefficient of friction and N+1 the load index [22]. In

these adjusts, the calculated R^2 was in the range of the 0.96 and 0.999.

3.5.2 Effect of the cell size in the friction coefficient

For this analysis, a group of foams, which have similar surface free energies and the same type of structure (closed-cell) was selected. This group was the *Plastazotes* foams. It should be noted that the Young's modulus is dependent on the cell size, so it was not possible to fix this parameter (Table 3).

The cell structure of the different Plastazote foams are given in figures 6, 7 and 8. Two different magnifications are presented: a lower one, to visualize the cells and to determine their radius, and a higher one to access the thickness of the cell walls.

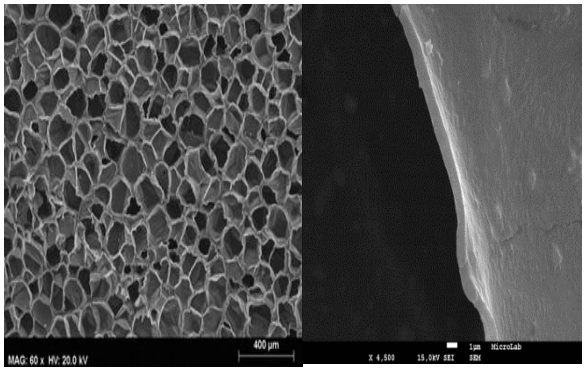

Figure 6. Photomicrograph of the white *Plastazote* foam with different magnifications

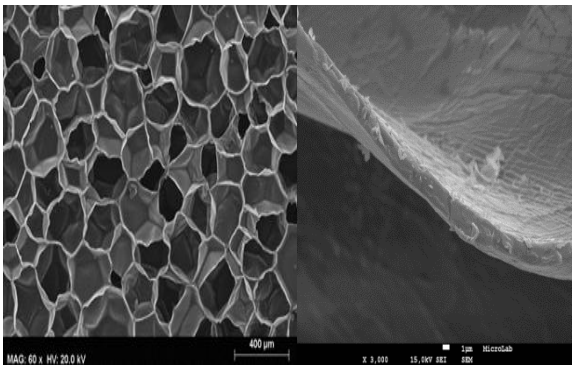

Figure 7. Photomicrograph of the normal clear *Plastazote* foam with different magnifications

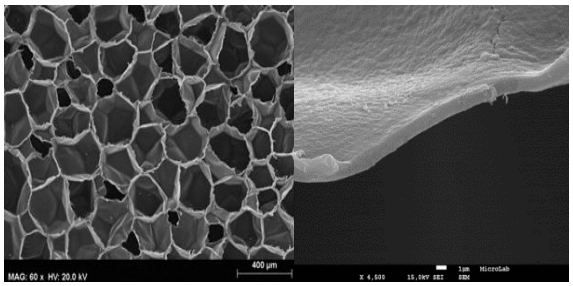

Figure 8. Photomicrograph of the perforated clear *Plastazote* foam with different magnifications

The figure 9 shows the evolution of the friction coefficient with the applied normal loads to *Plastazote* foams (at the left) and the results of the potential regression (at the right).

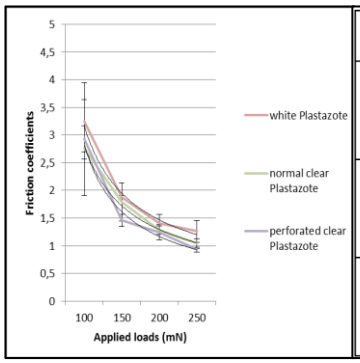

Foams	$\mu = k * Fn^N$
white Plastazote	$y = 3{,}1661x^{-0{,}7}$ $R^2 = 0{,}9889$
normal clear Plastazote	$y = 2{,}8185x^{-0{,}71}$ $R^2 = 0{,}9963$
perforated clear Plastazote	$y = 2{,}8194x^{-0{,}802}$ $R^2 = 0{,}9783$

Figure 9. Evolution of the friction coefficient with the applied normal loads to *Plastazote* foams (at the left) and the results of the potential regression (at the right).

From this analysis was concluded that the greater the cell size, the lower the friction coefficient, which is in agreement with the literature [23]. In fact, white *Plastazote* that has a much lower cell size than the normal and perforated clear *Plastazotes*, showed higher friction coefficients for all the normal applied tested forces.

This result is explained by the dependence of the contact area with the foam cell size. The number of ribs and cell walls of the foam increases with decreasing of cell size, and therefore, there will be more points of

contact between the foam and the skin, leading to a higher friction. In fact, the highest friction coefficient was obtained for white *Plastazote* with a contact area value of 0.017 cm^2 per cm^2 geometric area, while the lowest friction coefficients values were obtained for the normal and perforated *Plastazotes* with contact areas of 0.012 cm^2 to 0.013 cm^2 respectively.

Table 3. Cell radius, relative density and load-dependent coefficient of friction for the *Plastazote* foams

Foams	Cell radius (µm)	Relative density (ρ / ρs)	Load-dependent coefficient of friction (k)
white Plastazote	78 ± 8	0.11	k= 3.17
perforated clear Plastazote	127 ± 18	0.06	k= 2.82
normal clear Plastazote	133 ± 21	0.05	k= 2.82

As it is expected the evolution of the friction coefficient with the relative density of foams showed the same trend than the friction coefficient with the cell size. In fact these two parameters are dependent.

3.5.3 Effect of the surface free energy in the friction coefficient

For all the seventeen tested samples just two foams showed, same structure, similar cell size and Young's modulus with very different values of surface free energy: these foams were EVA and geriatric EVA (closed cell structure) (Table 4). For this analysis it was concluded that the friction coefficient depends on the surface free energy. Eva sample with highest value of surface free energy had the highest friction values. This result suggests that the surface free energy is related to the adhesion forces between the contacting sliding surfaces.

Table 4. Surface free energy and load-dependent coefficient of friction for the EVA foams

Foams	Surface free energy (mJ/m^2)	Load-dependent coefficient of friction (k)
Eva	43 ± 1	k= 3.48
Geriatric Eva	11 ± 2	k= 1.22

The polarity seems to affect the friction coefficients. From the analysis of figure 10, it was observed that the foams with the highest polarity showed the lowest load-dependent coefficient of friction (k), namely *Geriatric* Eva and Polyurethanes. More studies are needed to clarify this aspect.

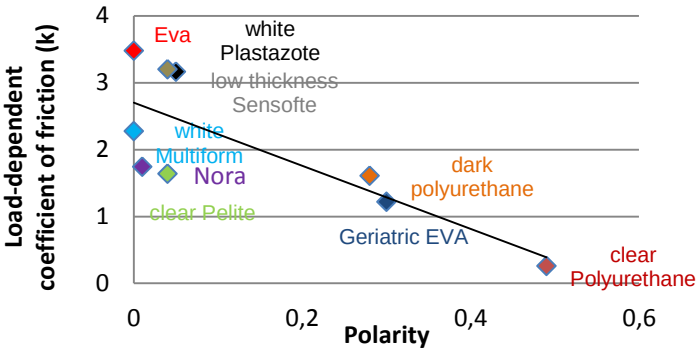

Figure 10. Representative graph of load-dependent coefficient of friction (k) according to the polarity

3.5.4 Effect of Young's modulus in the friction coefficient

The Young's Modulus is affected by the type of cell structure, cell size and wall thickness. Thus, it is not possible to fix these parameters independently.

To evaluate the effect of the Young's Modulus on the friction coefficient, the behavior of foams with similar surface free energy was compared. Two groups of foams with surface free energies close to 21.5 mJ/m^2 and 27.6 mJ/m^2 were constituted (Figure 11).

It can be observed that in both cases that the friction coefficient increases with the decrease of the Young's Modulus. This behavior shall be related with the amount of deformation of the foams in the elastic contact: lower Young's Modulus leads to higher deformation at the contact and therefore to a higher contact area, which origins a higher adhesion and a higher friction coefficient.

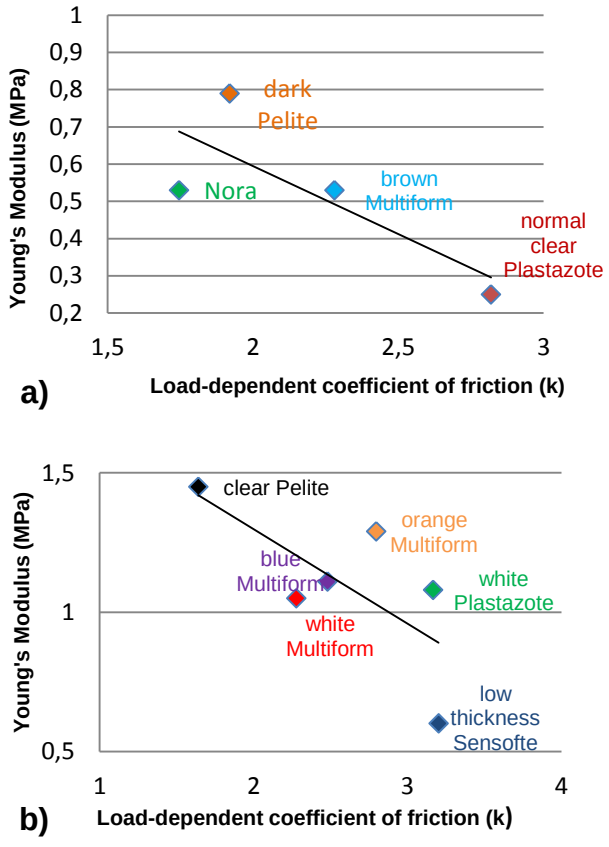

Figure 11. Representative graph of the Young's modulus according to the load-dependent coefficient of friction (k), for foam groups with average surface free energies close to a) 21.5 mJ/m^2 and b) 27.6 mJ/m^2

4. CONCLUSIONS

In order to evaluate the effect of the structure, surface energy and mechanical properties on the friction coefficient between artificial skin and orthopedic foams, seventeen commercial foams were selected, characterized and the friction coefficient determined. The results showed that the friction coefficient depends on the:

- Normal applied load: the friction coefficient decreases with the increase of the normal applied loads.
- Cell size: the friction coefficient decreases with the increases of the cell size.
- Surface free energy: the friction coefficient decreases with the decrease of the surface free energy.
- Young's Modulus: the friction coefficient decreases with the increase of the Young's Modulus.

REFERENCES

[1] D. W. Koenig, B. Dvoracek e R. Vongsa, "In vitro prediction of in vivo skin damage associated with the wiping of dry tissue against skin," *Skin Research and Technology,* vol. 19, pp. 453-458, 2012.

[2] "IMS.inc Empowering Product Development," [Online]. Available: http://www.ims-usa.com/vitro-skin. [Acedido em 2015].

[3] "IMS In Vitro SPF/UVA Protocol for use with VITRO-SKIN® Substrate," [Online]. Available: http://www.ims-usa.com/protocol. [Acedido em

2015].

[4] C. F. Pina, N. Patas, J. Canhoto, R. Cláudio, S. M. Olhero, A. P. Serro, A. C. Ferro e M. Guedes, "Tribological behaviour of unveneered and veneered lithium disilicate dental material," *Mechanical behavior of biomedical lmaterials,* vol. 53, pp. 226-238, 2015.

[5] B. Bhushan, S. Chen e S. Ge, "Friction and durability of virgin and damaged skin with and without skin cream treatment using atomic force microscopy," *Beilstein Journal of Nanotechnology,* vol. 3, p. 731–746, 2012.

[6] W. Tang e B. Bhushan, "Adhesion, friction and wear characterization of skin and skin cream using atomic force microscope," *Colloids and Surfaces B: Biointerfaces,* vol. 76, p. 1–15, 2010.

[7] A. Elkhyat, P. Agache, H. Zahouan e P. Humbert, "A new method to measure in vivo human skin," *International Journal of Cosmetic Science,* vol. 23, pp. 347-352, 2001.

[8] A. Elkhyat, C. Courderot-Masuyer, T. Gharbi e P. Humbert, "Influence of the hydrophobic and hydrophilic characteristics of sliding and slider surfaces on friction coefficient: in vivo human skin friction comparison," *Skin Research and Technology,* vol. 10, p. 215–221, 2004.

[9] A. Mavon , H. Zahouani, D. Redoules, P. Agache, Y. Gall e P. Humbert , "Sebum and stratum corneum lipids increase human skin surface free energy as determined from contact angle measurements: A study on two anatomical sites," *Colloids and Surfaces B: Biointerfaces,* vol. 8, pp. 147-155 , 1997.

[10] "All about plastic molding," D & M Plastics.Inc, [Online]. Available: http://www.plasticmoulding.ca/polymers/polyethylene.htm. [Acedido em 2015].

[11] "Material Properties Database," [Online].Available:http://www.makeitfrom.com/material-properties/Low-Density-Polyethylene-LDPE/. [Acedido em 2015].

[12] E. Linul, L. Marsavina, T. Voiconi e T. Sadowski, "Study of factors influencing the mechanical properties of polyurethane foams under dynamic compression," *Journal of Physics :Conference Series,* vol. 451, 2013.

[13] D. P. Subedi, "Contact Angle Measurement for The Surface Characterization of Solids," *The Himalayan Physics,* vol. 2, pp. 1-4, 2011.

[14] D. Pappas, C. Copeland e R. Jensen, "Wettability Tests of Polymer Films and Fabrics and Determination of Their Surface Energy by Contact-Angle Methods," Março 2007. [Online]. Available:http://www.researchgate.net/publication/235080831_Wettability_Tests_of_Polymer_Films_and_Fabrics_and_Determination_of_Their_Surface_Energy_by_ContactAngle_Methods. [Acedido em 2015].

[15] C. M. Mate, Tribology on the Small Scale: A bottom up approach to friction, lubrication, and wear, Oxford University Press, 2008, pp. 63-78.

[16] W. Tang, S.-r. Ge, H. Zhu, X.-c. Cao e N. Li, "The Influence of Normal Load and Sliding Speed on Frictional Properties of Skin," *Bionic Engineering,* vol. 5, p. 33−38, 2008.

[17] S. Derler, L. C. Gerhardt, A. Lenz, E. Bertaux e M. Hadad, "Friction of human skin against smooth and rough glass as a function of the contact pressure," *Tribology International,* vol. 42, p. 1565–1574, 2008.

[18] S. Derler, U. Schrade e L. C. Gerhardt, "Tribology of human skin and mechanical skin equivalents in contact with textiles," *Wear,* vol. 263, p. 1112–1116, 2007.

[19] A. F. El-Shimi, "In vivo skin friction measurements," *J. Soc. Cosmet, Chem,* vol. 28, pp. 37-51, 1977.

[20] K. C. Ludema, Friction, Wear, Lubrication: A Textbook in Tribology, CRC Press, 1996, pp. 35-81.

[21] B. Zappone , K. J. Rosenberg e J. Israelachvili, "Role of nanometer roughness on the adhesion and friction of a rough polymer surface and a molecularly smooth mica surface," *Tribology Letters,* vol. 26, pp. 191-201, 2007.

[22] M. J. Adams, B. J. Briscoe e S. A. Johnson, "Friction and lubrication of human skin," *Tribology Letters,* vol. 26, pp. 239-253, 2007.

[23] R. Landers, R. Hubel e R. Borgogelli, "The Importance of Cell Structure for Viscoelastic Foams," em *Polyurethanes Technical Conference*, Orlando, Florida, 2007.